Available online at www.sciencedirect.com

SciVerse ScienceDirect

Ceramics International 39 (2013) 5069–5075

CERAMICS INTERNATIONAL

www.elsevier.com/locate/ceramint

A comparative study of $Sr_{0.7}Ba_{0.3}Nb_2O_6$ relaxor ferroelectric ceramics prepared by conventional and microwave sintering techniques

Jinglei Li*, Yongping Pu, Zhuo Wang, Jie Dai

School of Materials Science and Engineering, Shaanxi University of Science and Technology, Shaanxi Xi'an 710021, China

Received 28 September 2012; received in revised form 23 November 2012; accepted 1 December 2012
Available online 8 December 2012

Abstract

$Sr_{0.7}Ba_{0.3}Nb_2O_6$ (SBN70) ceramics were prepared by conventional sintering (CS) and microwave sintering (MWS) techniques. High-density ceramics were obtained by the MWS method in 2 h of cycle time, whereas it took 14 h by the CS method. Samples prepared by both sintering techniques showed single phase formation according to XRD results. It was observed that MWS SBN70 ceramics showed better densification and more uniform grain size than those of CS samples. The dielectric characteristics of both samples showed diffuse phase transition phenomenon features, which was confirmed by linear fitting of the modified Curie–Weiss law. Besides, the relaxor ferroelectric properties of both samples followed the Vogel–Fulcher relationship well. The value of spontaneous polarization (P_s) and the P–E hysteresis loop for MWS samples were significantly higher and slimmer than those of the CS samples, respectively.

Keywords: Microwave sintering; Relaxor ferroelectric; Curie–Weiss law; Vogel–Fulcher relationship

1. Introduction

$Sr_xBa_{1-x}Nb_2O_6$ (SBN, where $0.25 \leq x \leq 0.75$) ceramics are ferroelectric materials with tungsten bronze structures, which have excellent electro-optic [1–3], pyroelectric [4–6], photorefractive [7–9], and piezoelectric [3] properties. In the past decades, SBN has received considerable attention as a candidate for lead-free electroceramics. Although single crystal SBN has superior properties to those of polycrystalline SBN, the high costs and complicated fabrication process limit its applications. Therefore, the achievement of full densification with a uniform microstructure of polycrystalline SBN ceramics is greatly desirable, which will benefit from lower cost and the easier fabrication process. However, as is well known, the sintering temperature for SBN ceramics is higher than 1350 °C, which can lead to abnormal growth and the generation of crack [10–14]. At present, the main solutions to avoid abnormal grain growth of SBN are two-step sintering method and adding additives. The disadvantages of the two-step sintering method are the high sintering temperature and the time-consuming complicated manufacturing process. In addition, low dielectric constant of SBN and high dielectric loss are always caused by the adding additives [15].

Microwave processing for preparing ceramic materials has been investigated in the past decade by many researchers. The increasing interest in microwave processing over conventional processing method is due to the fact that the electromagnetic wave interacts with ceramic materials leading to volumetric heating by dielectric loss, which will enhance the sintering process, decrease densification temperature, improve microstructure uniformity and the product properties as well. Compared with the conventional heating method, this unique heating method has also the potential for saving energy and cutting cost [16].

In this study, $Sr_{0.7}Ba_{0.3}Nb_2O_6$ (SBN70) ceramics were prepared by conventional sintering (CS) and microwave sintering (MWS) techniques. A comparison of different methods on the microstructure, dielectric properties, and relaxor ferroelectric properties is explained and discussed.

2. Experiment procedure

The starting materials of reagent grade $SrCO_3$ (99.95%), $BaCO_3$ (99.95%) and Nb_2O_5 (99.95%) powders were

*Corresponding author. Fax: +86 18792815467.
E-mail address: lilei19871003@yahoo.com.cn (J. Li).

0272-8842/$ - see front matter © 2012 Elsevier Ltd and Techna Group S.r.l. All rights reserved.
http://dx.doi.org/10.1016/j.ceramint.2012.12.001

weighed according to the nominal composition of $Sr_{0.7}Ba_{0.3}Nb_2O_6$. The weighed powders were added into a ball milling jar, and milled for 2 h in distilled water with ZrO_2 media. After drying, the mixture was calcined at 1200 °C for 6 h in a high-purity alumina crucible kept in a conventional furnace. The calcined powders were ball milled for 24 h and sieved again. The prepared powders were mixed with 5 wt% polyvinyl alcohol (PVA) solution and then pressed into pellets with a diameter of 13.6 mm under 10 MPa pressure. The disks were divided into two series. One set of series green bodies were sintered by the conventional method, which were sintered in a simple silicon carbide muffle furnace (KSL1700, Hefei Kjmt, China) at 1350 °C for 2 h with a heating and cooling rate of 3 °C/min. Prior to microwave sintering, another set of green bodies was annealed in air at 600 °C for 3 h in order to remove adsorbed water and organic compounds, which was then sintered at 1300 °C using a microwave sintering furnace for 30 min and the total cycle time was 2 h. The microwave furnace in this study consisted of 2.45 GHz magnetrons with maximum power of 3 kW (Raptor, Shanghai PreeKem, China). The ceramics samples were placed on a high-purity aluminum oxide plate surrounded by a hollow silicon carbide cylinder, which was used to enhance microwave heating efficiency and develop temperature homogeneity. The temperature–time sintering profile for CS and MWS is shown in Fig. 1. The crystal phase of the sintered ceramics was characterized by powder X-ray diffraction (XRD). A scanning electron microscope (SEM; Jeol, JSM-5400) was used for the microstructure observation. The ceramics with conducting silver paste were fired at 600 °C for 0.5 h for a good contact. The dielectric response of pellet ceramics was measured by an Agilent E4980A with temperature controller range from room temperature to 200 °C. *P–E* hysteresis loops were observed by an automated *P–E* loop tracer (M/s AR Imagetronics, India) based on modified Sawyer–Tower circuit.

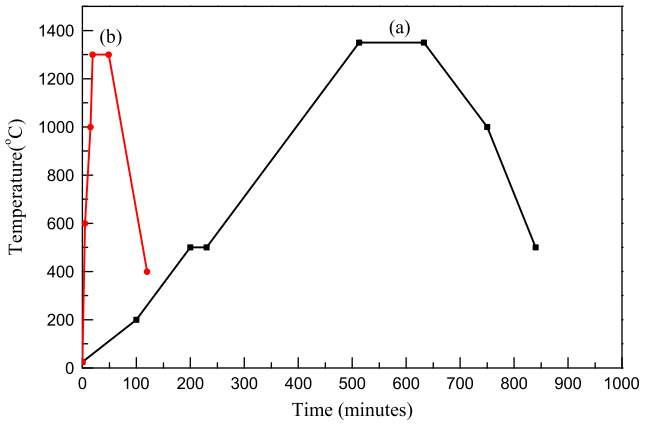

Fig. 1. Comparison of time–temperature sintering profile for (a) CS and (b) WMS SBN70 samples.

3. Results and discussion

The XRD patterns for (a) CS and (b) MWS SBN70 samples are shown in Fig. 2. Both ceramics are of tetragonal tungsten bronze (TB) structure.

Fig. 3 shows the scanning electron microscope (SEM) images of CS and MWS SBN70 samples. Crack and

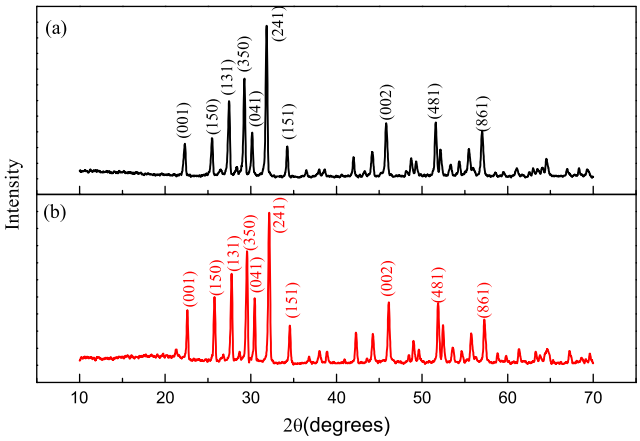

Fig. 2. XRD patterns for (a) CS and (b) MWS SBN70 samples.

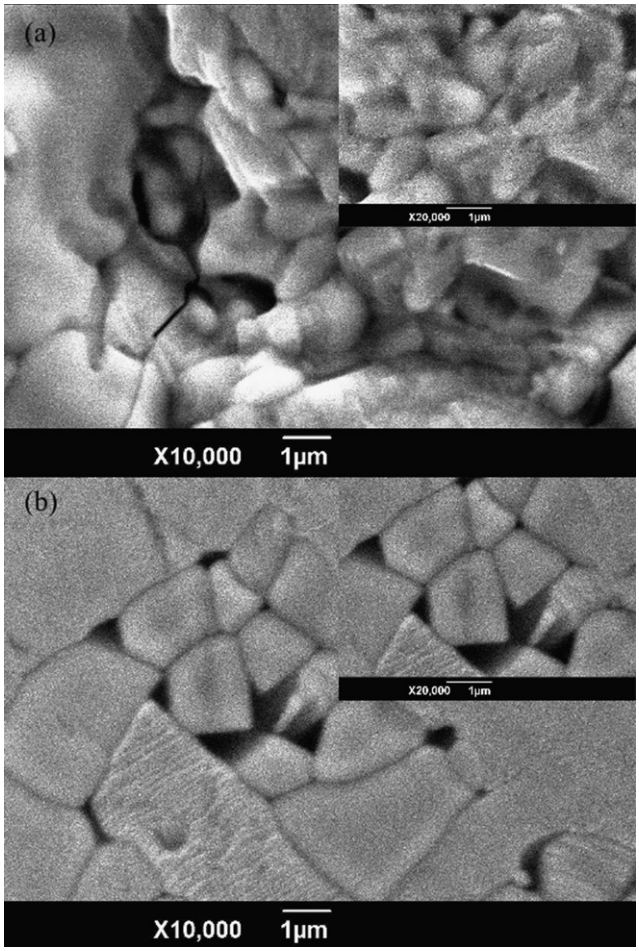

Fig. 3. SEM images for (a) CS and (b) MWS SBN70 samples.

inhomogeneous grain size are clearly observed for CS samples in Fig. 3(a). However, as shown in Fig. 3(b), MWS SBN70 samples obtained at 1300 °C showed uniform grain size and denser microstructure. In addition, it is important to note that the grain size of MWS SBN70 samples is larger than that of CS samples. This could be attributed to the fast grain growth and accelerated densification caused from the reduction of activation energy because of the interaction between the high electromagnetic fields and ceramic material [17].

Fig. 4 shows the dielectric constant and dielectric loss as a function of temperature measured at various frequencies. The relaxor behavior for both CS and WMS samples could be clearly observed. The maximum of dielectric constant and dielectric loss shift to higher temperatures with increasing frequency. The relaxor behavior is partly caused by the A Sites ions disorder. As far as we know, $Sr_xBa_{1-x}Nb_2O_6$ compounds ($0.25 \le x \le 0.75$) have TB structure with a unit-cell formula of $A1_2A2_4C_4B1_2B2_8O_{30}$, which is developed from the perovskite type structure by tilting the oxygen octahedral in such a way that the layers of [BO_6] octahedra sharing the corners form three types of voids: square A1, pentagonal A2, and triangular C channels. In the tungsten–bronze structure, the A1 positions are occupied by only Sr^{2+} and the A2-sites are filled with by both Sr^{2+} and Ba^{2+}, whereas the C sites are usually empty. There are only five Sr and Ba atoms for six A1 and A2 positions. As a result, one of the A-sites remains unoccupied and the missing charge on these vacancies is the source of random fields (RFs) [18]. Therefore the ion disorder in the unit cell could be the reason for the appearance of the frequency dispersion. Simultaneously, it was also observed that the peak values of dielectric constant and dielectric loss of WMS samples are higher than those of the CS samples.

It is well known that the classical ferroelectrics follow the Curie–Weiss law above Curie temperature (T_C) expressed by the following relationship:

$$\frac{1}{\varepsilon} = \frac{(T - T_C)}{C} \tag{1}$$

where T_C is the Curie–Weiss temperature and C is the Curie–Weiss constant. Fig. 5 shows the inverse of dielectric constant (ε) as a function of temperature for both samples, and the line is fitted with Eq. (1). The fitting parameters are shown in Table 1. An empirical parameter ΔT_m, defined as $\Delta T_m = T_{dev} - T_m$, is often used as a measurement of the degree of the deviation from the Curie–Weiss laws. Here, T_{dev} is deviated Curie–Weiss temperature. The values of T_{dev} for conventional and microwave sintered samples are given in Table 1.

Considering the signal of diffuse characteristic, the broaden dielectric peaks illustrate a typical relaxor behavior where the maximum dielectric constant electric constant decreases and T_C shifts to high temperature with the increase of frequency, indicating a diffuse phase transition (DPT). The DPT can be described by the modified Curie–Weiss law [19–21]

$$\frac{1}{\varepsilon} - \frac{1}{\varepsilon_{max}} = \frac{(T - T_C)^{\gamma}}{C} \tag{2}$$

where ε is the dielectric constant, T is the temperature, ε_{max} is the maximum value of ε at $T = T_C$, C is the modified Curie–Weiss constant and γ is a measurement of diffusivity, the material with $\gamma = 1$ fitting normal ferroelectric behavior, with $\gamma = 2$ showing a complete disordered system, and between 1 and 2 indicating diffuse ferroelectric characteristics. Fig. 6 shows the relationship between $\ln(1/\varepsilon - 1/\varepsilon_{max})$ and $\ln(T - T_C)$ for CS and WMS SBN70 ceramics. It is found that the diffuse

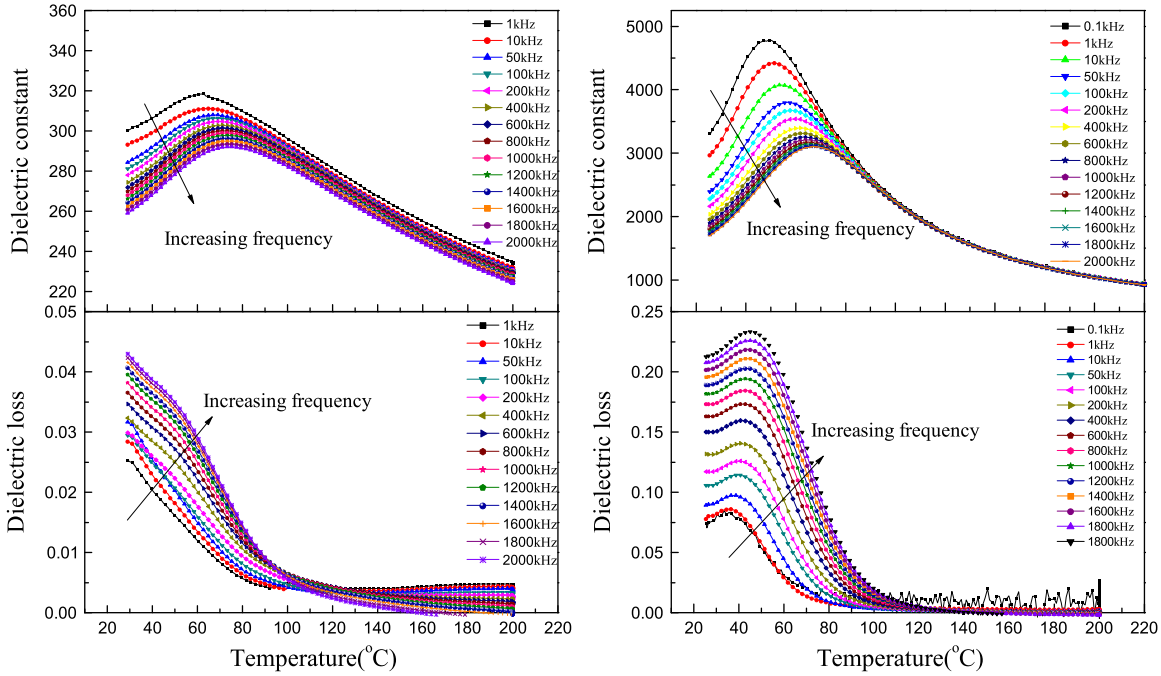

Fig. 4. Temperature dependence of dielectric constant and dielectric loss measured at different frequencies for (a) CS and (b) WMS SBN70 ceramics.

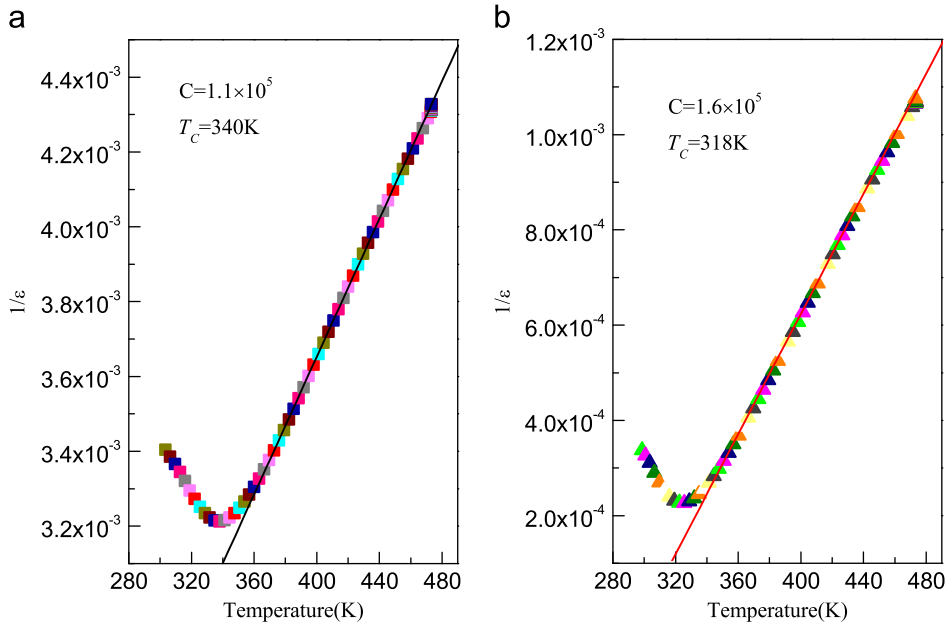

Fig. 5. Inverse of dielectric constant (ε) as a function of temperature for (a) CS and (b) WMS SBN70 ceramics.

Table 1
Physical and electrical parameters of conventional and microwave sintered samples.

	Conventional	Microwave
Sintering temperature (°C)	1350	1300
Soaking time (h)	2	0.5
Total cycle time (min)	840	120
Peak dielectric constant	317	4423
Peak dielectric loss	0.030	0.086
Curie constant	1.1×10^5	1.6×10^5
T_0 (K)	340	318
γ	1.66	1.68
ΔT_m (K)	31	32
ΔT_{dif} (K)	51	11
ΔT_{relax} (K)	10	9
Frequency f_0 (Hz)	5.4×10^8	5.9×10^8
Activation energy E_a (eV)	0.011	0.013
Freezing temperature (K)	326.3	313

exponents of both SBN70 ceramics are close to 2, confirming a typical diffuse ferroelectric behavior [22]. This could be attributed to the short-range correlation among the nanopolar domains [23]. In addition, the diffuseness of the phase transition can also be described by an empirical parameter ΔT_{dif}, defined as

$$\Delta T_{dif} = T_{0.9\varepsilon_m(100\ Hz)} - T_{\varepsilon_m(100\ Hz)} \quad (3)$$

i.e. the difference between $T_{0.9\varepsilon m(100\ Hz)}$ (the temperature corresponding to 90% of the dielectric constant (ε_m) at higher temperature side) and $T_{\varepsilon m(100\ Hz)}$. The value of ΔT_{dif} was found to be 51 K and 11 K for CS and MWS samples, respectively. It shows that the less diffusive nature of microwave sintered SBN70 ceramics as compared with conventional ones.

On the other hand, the degree of relaxation behavior (frequency range 100 Hz–100 kHz) could be described by a parameter ΔT_{relax}, which is defined as

$$\Delta T_{relax} = T_{\varepsilon_m(100\ kHz)} - T_{\varepsilon_m(100\ Hz)} \quad (4)$$

The values of ΔT_{relax} for both samples are shown in Table 1. Compared with the CS samples, the MWS samples show less degree of relaxation behavior. Combined with above ΔT_m, γ, ΔT_{relax}, and ΔT_{dif} results, the following can be concluded: (i) dielectric behavior of SBN70 ceramics follows the Curie–Weiss law when the temperature is higher than $T_{\varepsilon m}$; (ii) ΔT_{dif} and ΔT_{relax} show significant diffuseness of the phase transition and some frequency dispersion; and (iii) the value of γ is close to 2, indicating that both samples have typical ferroelectric relaxor behavior [24].

The frequency dispersion near dielectric maxima in relaxor ferroelectrics can be attributed to the distribution of relaxation times. A large number of theoretical models have been proposed to understand the diffusiveness of the dispersion. Among these the Vogel–Fulcher model is considered to be the most successful mathematical representation for the divergent nature of relaxation time below a certain temperature [18]. The observed frequency dependence of T_m could be described by the Vogel–Fulcher equation [25,26] as

$$f = f_0 e^{-E_a/(K_B(T_C - T_f))} \quad (5)$$

where f_0 is the pre-exponential term, E_a is the activation energy from polarization fluctuation of an isolated micropolar region, T_C is the temperature of the maximal dielectric constant, K_B is the Boltzmann constant, and T_f is the Vogel–Fulcher temperature, i.e., the static freezing temperature.

Fig. 7 shows inverse of Curie temperature T_C as a function of measurement frequency for both CS and WMS SBN70

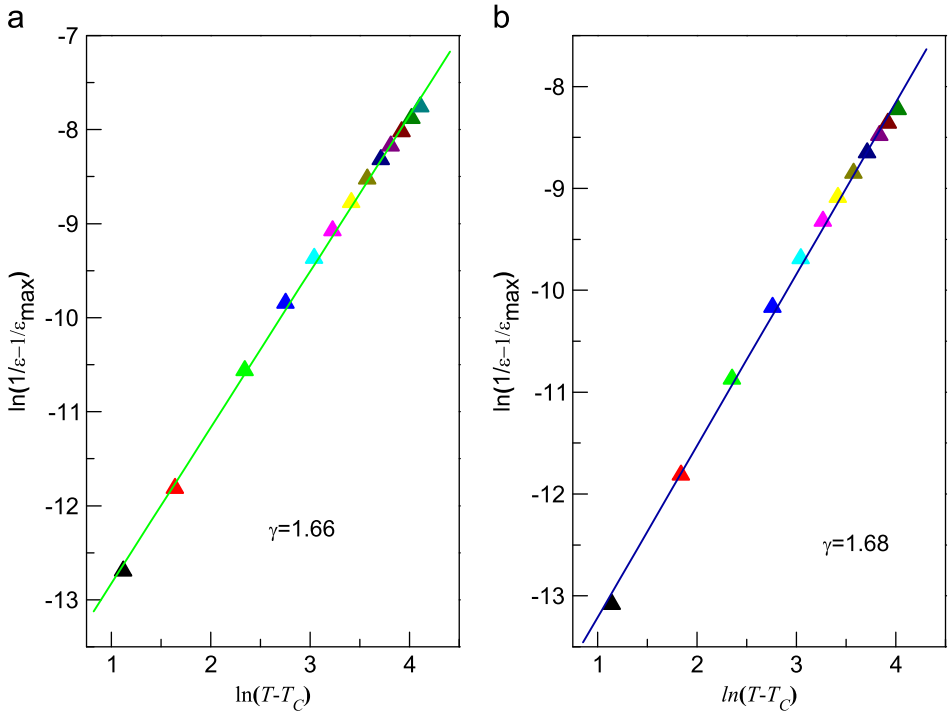

Fig. 6. Relationship between $\ln(1/\varepsilon - 1/\varepsilon_{max})$ and $\ln(T–T_C)$ for (a) CS and (b) WMS SBN70 ceramics.

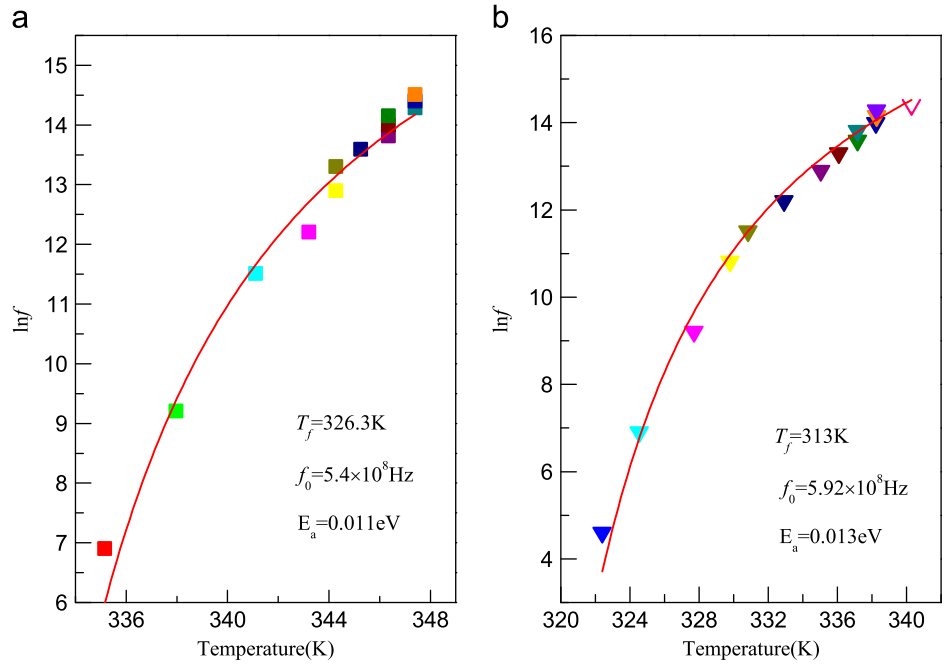

Fig. 7. Inverse of Curie temperature T_C as a function of measurement frequency for (a) CS and (b) WMS SBN70 ceramics.

ceramics. The fitting parameters (T_f, f_0 and E_a) in Vogel–Fulcher relationship are summarized in Table 1. SBN70 ceramics show a typical spin-glass-like dielectric relaxation behavior. The glassy behavior nature is attributed to the randomly oriented dipolar and electric fields [27]. The relaxation distribution is strongly broadened to T_f.

The polarization levels versus applied electrical field (P–E) hysteresis loops measured at room temperature are shown in Fig. 8. The values of spontaneous polarization (P_s) and the P–E hysteresis loop for MWS samples were significantly higher and slimmer than those of the CS samples, respectively.

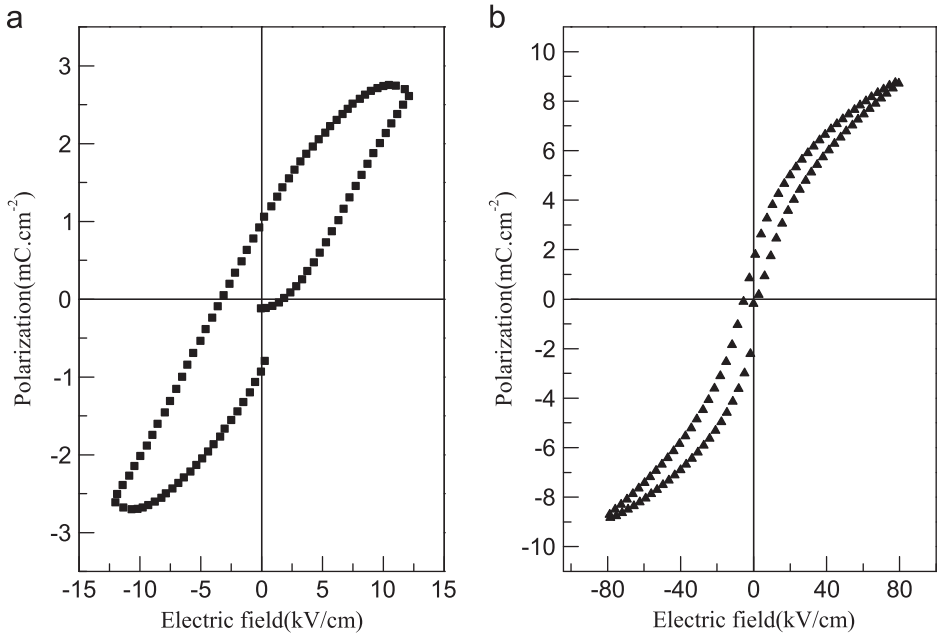

Fig. 8. *P–E* hysteresis loops for (a) CS and (b) WMS SBN70 ceramics measured at room temperature.

4. Conclusions

Single-phase tungsten bronze structure was obtained via conventional and microwave sintering techniques. Uniform grains were achieved by the microwave sintering technique with lower sintering temperature and shorter soaking time compared to those of conventional process. Comparison and analysis on the dielectric characteristics and relaxor ferroelectric properties were systematically studied by empirical parameters calculated from the modified Curie–Weiss law and Vogel–Fulcher relationship. The value of spontaneous polarization (P_s) and the *P–E* hysteresis loop for microwave sintering samples were significantly higher and slimmer than those of the conventional sintering samples, respectively.

Acknowledgment

This research was supported by the National Natural Science Foundation of China (51072106, 51102159), the New Century Excellent Talents Program of Chinese Education Ministry (NCET-11-1042), Foundation of Shaanxi Educational Committee (12JK0447), International Science and Technology Cooperation Project Funding of Shaanxi Province (2012KW-06), the Academic Leaders Cultivation Program and Graduate Innovation Fund of Shaanxi University of Science and Technology.

References

[1] P.B. Jamieson, S.C. Abrahams, J.L. Bernstein, Ferroelectric tungsten bronze-type crystal structures. Barium strontium niobate $Ba_{0.27}Sr_{0.75}Nb_2O_{5.78}$, Journal of Chemical Physics 48 (1968) 5048–5057.

[2] P.V. Lenzo, E.G. Spencer, A.A. Ballman, Electro-optic coefficients of ferroelectrics strontium barium niobate, Applied Physics Letters 11 (1967) 23–24.

[3] K. Nagata, Y. Yamamoto, H. Igarashi, K. Okazaki, Properties of the hot-pressed strontium barium niobate ceramics, Ferroelectrics 38 (1981) 853–856.

[4] A.M. Glass, Investigation of the electrical properties of $Sr_{1-x}Ba_xNb_2O_6$ with special reference to pyroelectric detection, Journal of Applied Physics 40 (1969) 4699–4713.

[5] S.I. Lee, W.K. Choo, Modified ferroelectric high density strontium barium niobate ceramics for pyroelectric applications, Ferroelectrics 87 (1988) 209–212.

[6] A.M. Glass, Ferroelectric $Sr_{1-x}Ba_xNb_2O_6$ as a fast and sensitive detector of infrared radiation, Applied Physics Letters 13 (1968) 147–149.

[7] T. Imai, S. Yagi, K. Yamazaki, M. Ono, Effects of heat treatment on photorefractive sensitivity of Ce- and Eu-doped strontium barium niobate, Japanese Journal of Applied Physics 38 (1999) 1984–1988.

[8] E.L. Venturini, E.G. Spencer, P.V. Lenzo, A.A. Ballman, Refractive indices of strontium barium niobate, Journal of Applied Physics 39 (1968) 343–344.

[9] M.D. Ewbank, R.R. Neugaonkar, W.K. Cory, J. Feinbery, Photorefractive properties of strontium barium niobate, Journal of Applied Physics 62 (1987) 374–380.

[10] J. Takahashi, S. Nishiwaki, K. Kodaira, Sintering and microstructure for $Sr_{0.6}Ba_{0.4}Nb_2O_6$ ceramics, Ceramic Taransactions 41 (1994) 363–370.

[11] S. Nishiwaki, J. Takahashi, K. Kodaira, Effect of additives on microstructure development and ferroelectric properties of $Sr_{0.3}Ba_{0.7}Nb_2O_6$ ceramics, Japanese Journal of Applied Physics 33 (1994) 5477–5481.

[12] H.Y. Lee, R. Freer, The mechanism of abnormal grain growth in $Sr_{0.6}Ba_{0.4}Nb_2O_6$ ceramics, Journal of Applied Physics 81 (1997) 376–382.

[13] H.Y. Lee, R. Freer, Abnormal grain growth and liquid-phase sintering in $Sr_{0.6}Ba_{0.4}Nb_2O_6$ (SBN40) ceramics, Journal of Materials Science 33 (1998) 1703–1708.

[14] T.T. Fang, E. Chen, W.J. Lee, On the discontinuous grain growth of $Sr_xBa_{1-x}Nb_2O_6$ ceramics, Journal of the European Ceramic Society 20 (2000) 527–530.

[15] Q.I. Bing, Chen Guohua, Development of strontium barium niobate ceramics, Material Reviews 21 (2007) 20–23.

[16] M. Venkata Ramana, S. Roopas Kiran, N. Ramamanohar Reddy, K.V. Siva Kumar, V.R.K. Murthy, B.S. Murth, Investigation and characterization of $Pb(Zr_{0.52}Ti_{0.48})O_3$ nanocrystalline ferroelectric ceramics: by conventional and microwave sintering methods, Materials Chemistry and Physics 126 (2011) 295–300.
[17] N.A. Travitzky, A. Goldstein, O. Avsian, A. Singurindi, Microwave sintering and mechanical properties of Y–TZP/20 wt% Al_2O_3 composites, Material Science and Engineering A 286 (2000) 225–229.
[18] A.A. Bokov, Z.G. YE, Recent progress in relaxor ferroelectrics with perovskite structure, Journal of Materials Science 41 (2006) 31–52.
[19] V.V. kirrillow, V.A. Isupov, Relaxation polarization of $PbMg_{1/3}Nb_{2/3}O_3$ (PMN)—a ferroelectric with a diffused phase transition, Ferroelectrics 5 (1973) 3–9.
[20] Z.R. Liu, Y. Zhang, B.L. Gu, X.W. Zhang, The properties of frozen local polarization in relaxor ferroelectrics, Journal of Physics: Condensed Matter 13 (2001) 1133–1139.
[21] K. Uchino, S. Nomura, Critical exponents of the dielectric constant in diffused-phase-transition crystals, Ferroelectric 44 (1982) 55–61.
[22] A. Aoujgal, W.A. Gharbi, A. Outzourhit, A. Ammar, A. Tachafine, J.C. Carru, Relaxor behavior in $(Ba_{1-3x/2}Bi_x)(Zr_yTi_{1-y})O_3$ ceramics, Ceramics International 37 (2011) 2069–2074.
[23] D. Vichland, S.J. Jang, L.E. Cross, M. Wutting, Deviation from Curie–Weiss behavior in relaxor ferroelectrics, Physical Review B 46 (1992) 8003.
[24] Sandeep Mahajan, O.P. Thakur, D.K. Bhattacharya, K. Sreenivas, A comparative study of $Ba_{0.95}Ca_{0.05}Zr_{0.25}Ti_{0.75}O_3$ realxor ceramics prepared by conventional and microwave sintering techniques, Materials Chemistry and Physics 112 (2008) 858–862.
[25] H. Vogel, The law of the relation between the viscosity of liquids and the temperature, Physikalische Zeitschriften 22 (1921) 645–646.
[26] G.S. Fulcher, Analysis of recent measurements of the viscosity of glasses, Journal of the American Ceramic Society 8 (1925) 339–355.
[27] M. Adamczyk, A. Molak, Z. Ujma, The influence of axial pressure on relaxor properties of $BaBi_2Nb_2O_9$ ceramics, Ceramics International 35 (2009) 2197–2202.